15th Triennial World Congress, Barcelona, Spain

KALMAN FILTERING AND TORQUE SPECTRAL ANALYSIS FOR BROKEN BAR DETECTION IN INDUCTION MOTORS

Mario Eltabach, Ali Charara, Ismail Zein
HEUDIASYC UMR 6599 - LATIM
Université de Technologie de Compiègne
BP 20529
60205 Compiègne Cedex; France
email: mario.eltabach@utc.fr

Abstract: Rotor asymmetries in induction machines perturb many components such as, flux patterns and electromagnetic torque. The supervision of these signals enables early detection of such faults and help to machine diagnostic. This paper studies the detection of rotor imperfection by spectral analysis of the electromagnetic torque computed by two rotor flux estimators. In the first approach, the Kalman filter is used assuming to be known the mechanical velocity. The second approach uses Extended Kalman Filter (EKF) for speed estimation. Experimental results show the great capability of these methods to detect this type of faults. *Copyright C 2002 IFAC.*

Keywords: Induction machines, diagnostics, fault detection, Kalman algorithms.

1. INTRODUCTION

In many applications, motor failures can shut down an entire industrial process. Such unexpected shut downs have a cost, in terms of both time and money, which could be avoided by the use of some form of early warning system. In Large machines, broken rotor bars may occur due to high temperatures, poor end-ring joints and large centrifugal forces produced during transient operations such as startup. On-line monitoring of three phase induction machines is usually based on spectral analysis of electrical signature as the stator currents or the electromagnetic torque. Commercially available diagnostic systems identify characteristic spectral components, in order to aid an expert to evaluate the health of the machine. Rotor asymmetries such as the broken rotor bars contribute to the distortion of currents in rotating machines, these asymmetries give rises to sideband frequencies around the fundamental harmonic in the current spectrum. The main disadvantage of these signatures resides in load-dependent small frequency shifts in the spectrum, especially when the load is weak. That means that the extraction of the fault signature requires the dynamic to be large and the extraction method to be accurate (Kliman, 1992; Elkasabgy, 1992; Shoen & all, 1997; Benbouzid, 2000; Cardoso, 1993). Other studies, as in (Cruz & all 2000b), have proposed a spectral analysis of the current Park vector modulus, which takes advantage of the fact that the spectrum does not contain a fundamental component, but only relative frequencies directly linked to the fault, thus rendering these components easier to isolate.
Trzynadlowski (1999a), Stanislaw (1996), Cruz & all (1999a) study the spectral analysis of partial and total instantaneous powers. The spectrum of partial instantaneous powers contains a double fault signature: the first is shown by the appearance of components within the two lateral bands located around twice the fundamental frequency, while the second is shown at low frequencies by the appearance of components at the fault's characteristic frequencies. The spectrum of total instantaneous power, on the other hand, contains only one fault signature at low frequencies (Cruz & all 1999a).
Kral & all (2000) study the spectral analysis of the E.M.T (Electromagnetic Torque), computed from the stator flux estimation and stator current measurement. This method assumes the knowledge of the stator resistance value. However, the E.M.T can be deduced from the observed rotor flux using observers like Luenberger observer treated in (Eltabach & all 2001).
This article presents a fault detection method based on the spectrum analysis of the electromagnetic torque, which is obtained by rotor flux estimation. This estimation is obtained by two approaches using Kalman filtering applied to the stochastic second order model. The first approach assumes the mechanical velocity to be known, whilst the second approach uses extended filter for rotor flux and velocity estimation.
In this paper, section 2 reviews the second-order model of the induction motor, Kalman filter and EKF based on this model. Experimental results and a comparison between the two approaches are presented in section 3.

2. THEORETICAL DEVELOPMENT

The electromagnetic torque of an induction motor can be computed from certain known motor variables such as: stator currents and stator flux or stator currents and rotor flux. Stator flux can be computed using currents and voltages of the power supply.

Rotor flux, in other hand, can be computed from model-based observers such as Kalman filter. This estimation needs the knowledge of the machine parameters, currents, mechanical speed and voltages.

2.1. Rotor flux estimation using an open loop method and Kalman filter

To get a simple model for rotor flux and mechanical velocity, we consider the stator currents as input $U = [\, I_{sd}\ I_{sq}\,]^T$ and the stator voltages as output $Z = [V_{sd}\ V_{sq}\,]^T$. This model is an equivalent two-phase model deduced from Park transformation and presented in a d-q plan rotating at w_x. Consequently, the state vector (X) consists only of the rotor flux components: $X = [\Phi_{rd}\ \Phi_{rq}\,]^T$. With these assumptions, we obtain:

$$\dot{X} = AX + BU \quad (1)$$

$$Z = C(w_m)X + D(w_m)U + E\dot{U} \quad (2)$$

$$A = -\rho_r I - (w_x - w_m)J,\ B = R_r I,\ C = -\rho_r I + w_m J,$$
$$D = (R_s + R_r)I + L_{fs} w_x J,\ E = L_{fs} I$$

$$I = \begin{bmatrix} 1 & 0 \\ 0 & 1 \end{bmatrix} \text{ and } J = \begin{bmatrix} 0 & -1 \\ 1 & 0 \end{bmatrix},\ \rho_r = \frac{R_r}{L_r}\ w_m = P\Omega_m$$

R_s, R_r, L_{fs}, L_r P, Ω_m are respectively the stator resistance, rotor resistance, total leakage inductance rotor inductance, number of pair of poles and the mechanical velocity.

Since, in the first approach the mechanical velocity (w_m) is taken known, the mechanical frame is chosen as a reference frame for the electrical signals since the matrices of the state equation are constant. The estimation of the rotor flux in an open loop is obtained from the discrete-time solution of the equation (1) and given by (3):

$$\Phi_{(k+1)} = e^{-\rho_r T_e}\Phi_k + L_r(1 - e^{-\rho_r T_e})I_{sk}. \quad (3)$$

Indices k and $k+1$ mean the variables values taken at t_k and t_{k+1} respectively.

The fact that the state vector consists only of the rotor flux has a dual advantage. First, the reduction of the state dimension reduces the computational volume and complexity. Secondly, low rotor flux dynamic in this frame is easier to estimate: the second-order model has only real and slow poles.

The discrete-time model is obtained by integrating the state equation (1) over the sampling period Te:

$$X_{k+1} = e^{AT_e}X_k + \int_0^{T_e} e^{A(T_e - \tau)}BU(t_k + \tau)d\tau \quad (4)$$

Several methods are possible to compute the integral in (4), which depends on the input dynamic behavior over the interval $[t_k, t_{k+1}]$. By arranging equation (2) and by interpolating the model input vector U_k over the period T_e then estimation based discrete-time model in the mechanical reference frame (w_x=w_m) is defined by the following equations:

$$\begin{cases} X_{k+1} = A_d X_k + B_d U_k \\ Y_k = C_k X_k \end{cases} \quad (5)$$

$$A_d = e^{-\rho_r T_e} I,\ B_d = L_r(1 - e^{-\rho_r T_e})I$$
$$C_k = -\rho_r I + w_{m,k} J,\quad Y_k = Z_k - D(w_m)U_k - E\dot{U}_k$$

The numerical computation of the derivative of the stator current is the unique difficulty in the output equation of the second order model. It was performed by applying a low-pass filter to all signals to reduce noise effects.

The estimation of the rotor flux by the Kalman filtering can be resumed by the following equations:

$$\begin{cases} \hat{X}_{k+1/k+1} = \hat{X}_{k+1/k} + K_{K,k+1}(Y_{k+1} - \hat{Y}_{k+1/k}) \\ \hat{Y}_{k+1/k} = C_{k+1}\hat{X}_{k+1/k} \end{cases} \quad (6)$$

For more details on this estimator, one can referred to (Zein, 2000).

2.2. Rotor flux and mechanical velocity estimation by EKF

The stochastic extended model is obtained by combining the motor reduced-order model referred to the synchronous frame (w_s = 314 rd/s) and the mechanical velocity dynamic behavior, with the assumption that it is constant or varying slowly and finally by first order approximation of the discrete – time model:

$$\begin{cases} X_{e,k+1} = f(X_k, w_{m,k}) + W_{e,k} \\ Y_k = g(X_k, w_{m,k}) + V_k \end{cases} \quad (7)$$

With, $X_{e,k} = \begin{bmatrix} X_k & w_{m,k} \end{bmatrix}^T = \begin{bmatrix} \Phi_{rd} \Phi_{rq} w_{m,k} \end{bmatrix}^T$

$$f = \begin{bmatrix} A_{de}(w_{m,k})X_k + B_{de}U_k \\ w_{m,k} \end{bmatrix}$$

$$g(X_k, w_{m,k}) = C_k(w_{m,k})X_k$$

$$A_{de} = (1 - \rho_r T_e) - T_e(w_s - w_m)J$$
$$B_{de,k} = T_e R_r I$$
$$Q_{e,k} = E\{W_{e,k}W_{e,k}^t\},\ R_k = E\{V_k V_k^t\} \quad (8)$$

$W_{e,k}$ and V_k are the extended state and measurement noises respectively. We suppose that they are white, gaussian and zero mean noises. These noises are defined by their covariance matrices ($Q_{e,k}$, R_k). For simplicity, they are supposed to be diagonal matrices.

The EKF consists of two phases. First, the extended state is predicted according to the extended model given in (7).

$$\begin{cases} \hat{X}_{e,k+1/k} = f(\hat{X}_{k/k}, \hat{w}_{m,k/k}) \\ \hat{Y}_{k+1/k} = g(\hat{X}_{k+1/k}, \hat{w}_{m,k+1/k}) \end{cases} \quad (9)$$

Subsequently, this prediction is corrected by injecting the output estimation error:

$$\hat{X}_{e,k+1/k+1} = \hat{X}_{e,k+1/k} + K_{k+1}(Y_{k+1} - \hat{Y}_{k+1/k}) \quad (10)$$

The Kalman gain K is deduced from the properties of the stochastic model in order to minimize the variance of the estimation error. However, because

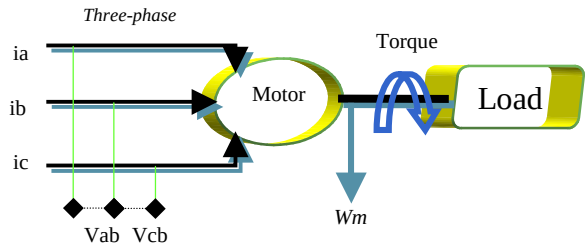

Fig.1. Experimental setup

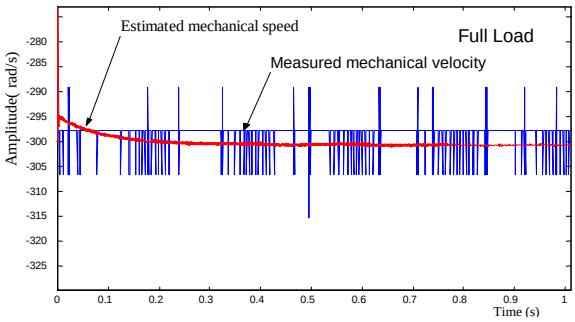

Fig.2. Comparison between estimated and measured mechanical speed. Motor with broken bar (full load)

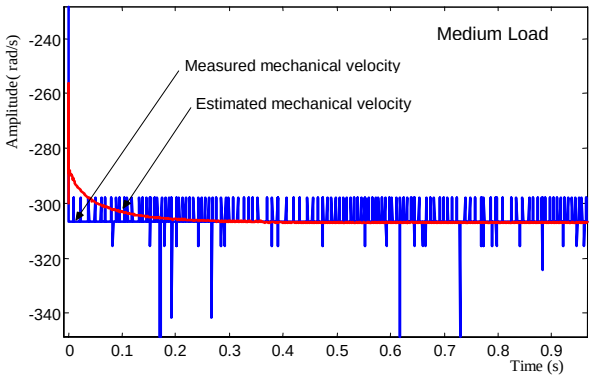

Fig.3. Comparison between estimated and measured mechanical velocity. Motor with broken bar (half load)

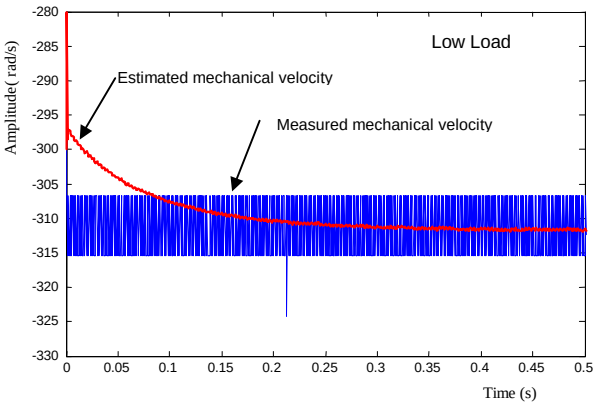

Fig.4. Comparison between Estimated and measured mechanical velocity. Motor with broken bar (Low Load)

the Kalman filter is a linear observer, the extended model must be linearised with respect to the estimated extended state.

$$\begin{cases} \tilde{X}_{e,k+1} = F_k \tilde{X}_{e,k/k} + W_{e,k} \\ \tilde{Y}_{k+1/k} = G_{k+1} \tilde{X}_{e,k+1/k} + V_{k+1} \end{cases} \quad (11)$$

With $\tilde{X}_e = X_e - \hat{X}_e$ the estimation error and with the following Jacobean matrices:

$$F_k = \left[\frac{\partial f(X_k, w_{m,k})}{\partial X_e}\right]_{X_e=\hat{X}_e} = \begin{bmatrix} A_{de}(\hat{w}_{m,k}) & J_x \\ 0 & 1 \end{bmatrix}$$

$$G_{k+1} = \left[\frac{\partial g(X_{k+1}, w_{m,k+1})}{\partial X_e}\right]_{X_e=\hat{X}_e} = \begin{bmatrix} C_{k+1} & J_y \end{bmatrix}$$

$$J_x = \left[\frac{\partial X_{k+1,i}}{\partial w_m}\right]_{X_e=\hat{X}_e} \text{ and } J_y = \left[\frac{\partial Y_{k+1,i}}{\partial w_m}\right]_{X_e=\hat{X}_e}$$

i=1,2

With the additional assumption that there is no correlation between the system noises and state error components, the original gain (the Kalman gain) and the covariance matrix of the estimation errors ($P_{e,l} = E\{\tilde{X}_{e,l} \tilde{X}^T_{e,l}\}, l = k/k, k+1/k \text{ and } k+1/k+1$) are given by:

$$P_{e,k+1/k} = F_k P_{e,k/k} F_k^T + Q_{e,k} \quad (12)$$

$$P_{Y,k+1/k} = G_{k+1} P_{e,k+1/k} G_{k+1}^T + R_{k+1} \quad (13)$$

$$K_{k+1} = P_{e,k+1/k} G_{k+1}^T P_{Y,k+1/k}^{-1} \quad (14)$$

$$P_{e,k+1/k+1} = P_{e,k+1/k} - K_{k+1} P_{Y,k+1/k} K_{k+1}^T \quad (15)$$

3. EXPERIMENTAL RESULTS

The experimental tests were carried out using the equipment described below (see Fig. 1):
1 - Motor: 220/380 V; 50 Hz; 1.1 kW; P=1.
2 - Motor electric parameters: R_s=11 Ω, R_r=3.75 Ω, L_{fs}=0.04H, L_r=0.47 H
3 - Three voltage sensors with insulation amplifiers
4 - Three current sensors (LEM)
5 - An incremental encoder position sensor (2048-point).

The measured signal sampling period is 0.7 ms (1428 Hz). The motor electric parameters were estimated correctly by an EKF using undamaged motor and optimal data for parameters estimation (Zein, 2000). The detection tests were performed with the equipment described above, first using an undamaged motor, and then one with one broken bar. In each case three different levels of load were used: full, medium, low which correspond to 100%, 60% and 22% of the nominal torque respectively.

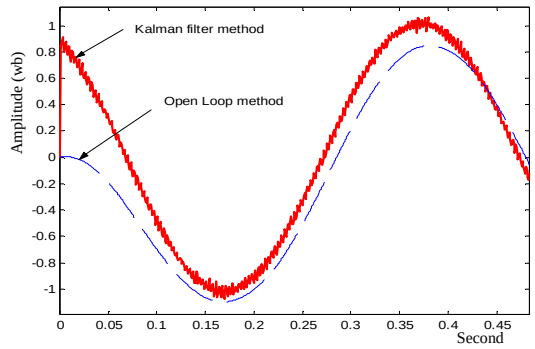

Fig.5. Comparison between estimated rotor flux d components, referred to the mechanical frame: Kalman filter and open loop model estimation.

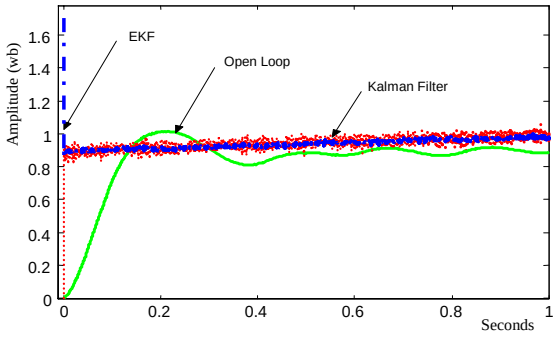

Fig.6. Comparison between estimated rotor flux d components, referred to the synchronous frame: Open Loop, Kalman filter and EKF Methods.

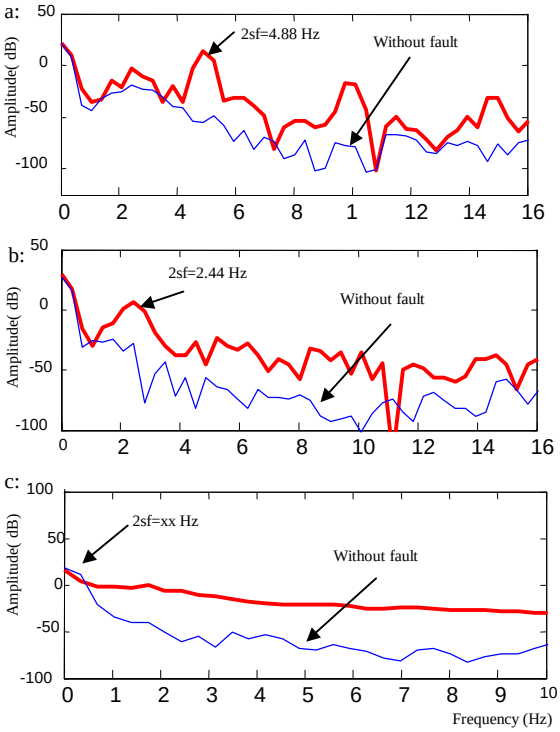

Fig.7 Torque spectrum with respect to the his mean value calculated from rotor flux in an open loop (Thick line: broken bar, thin line: without fault) for load levels: a. Full, b. Medium, c. Low

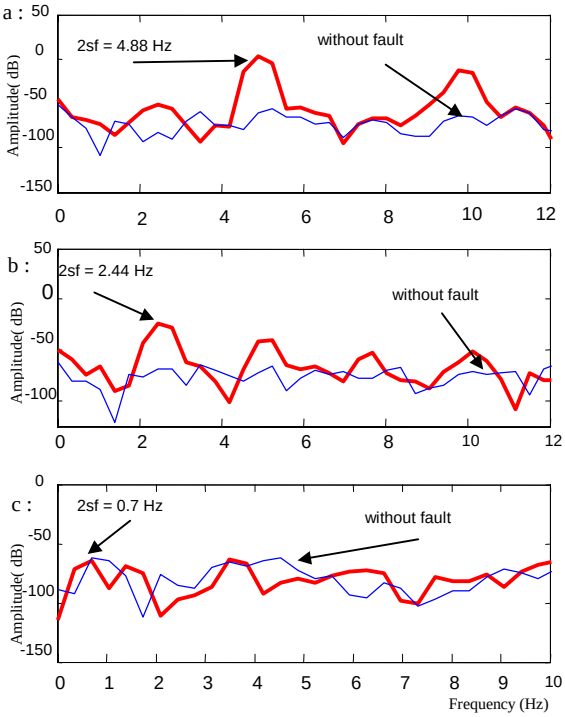

Fig.8. Estimated torque spectra with respect to its mean value, computed from estimated rotor flux by KF, (Thick line: broken bar, thin line: without fault) for load levels: a. full, b. medium, c. low

3.1 Estimation of the mechanical velocity and rotor flux components.

Fig.2,3,4 compare the estimated mechanical velocity by EKF based on the second-order model and the measured one in three different load levels (full, medium, low).

Table 1 shows a comparison between the estimated and the measured velocity mean values. Note that the velocity estimation error does not exceed 0.72 % (table1). Fig.5 shows estimation of the d component rotor flux referred to the mechanical frame, computed using two methods:

1-open loop (OL) method.

2-Kalman filter applied to the second order model.

In these two methods the mechanical velocity is assumed to be known. It is to be noted that the Kalman filter method has several advantages. Thus, the estimation dynamic behavior is much higher when the Kalman filtering is used. Fig.6 shows the "d" components of the rotor flux referred to the synchronous frame estimated using three methods: Open loop method, KF "Kalman filter" applied to the second order model and EKF method.

Table 1: Mean values of measured and estimated mechanical velocity by EKF (rad/s)

Load	Measured	Estimated
Full	298.4	300.5
Half	306.1	306.5
Low	311.5	311.3

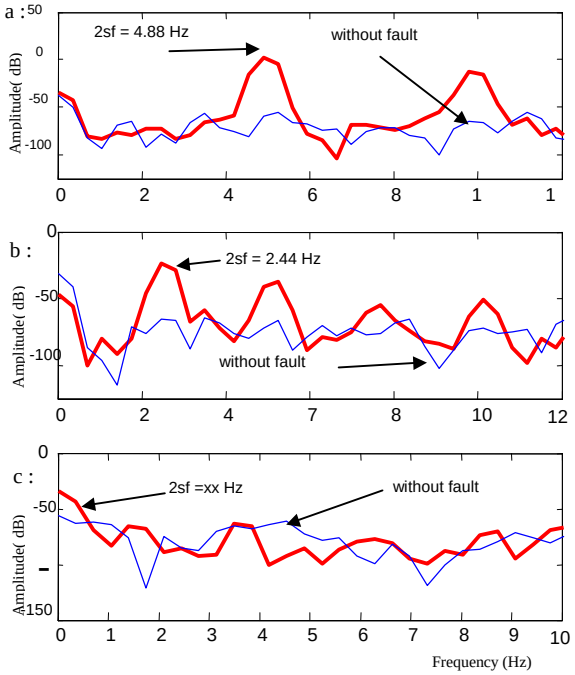

Fig.9. Estimated torque spectra with respect to its mean value, computed from estimated rotor flux by EKF, for load levels: a. full, b. medium, c. low. (Thick line: broken bar, thin line: without fault)

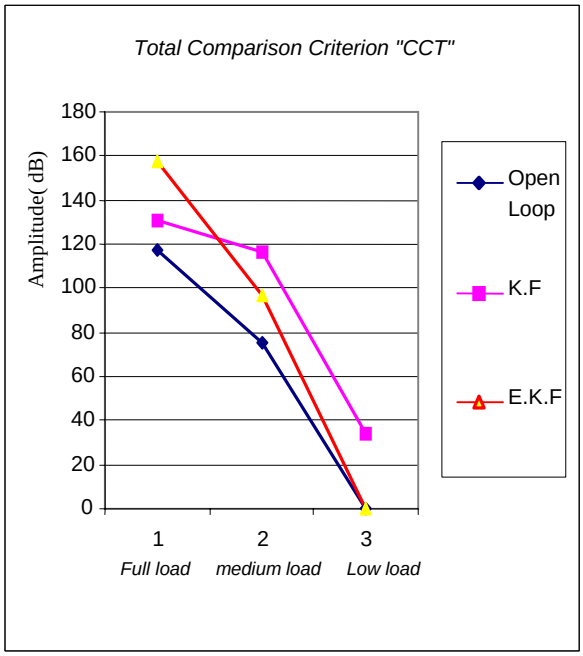

Fig. 10. Total Comparison criterion function of load levels

The "d" component is normally constant in the synchronous frame, as Fig.6 clearly shows.

3.2 Spectral analysis of the electromagnetic torque

The electromagnetic torque can be obtained by multiplying rotor flux and stator currents using the following formula:

$$C_{em} = \frac{3}{2} P\left(\Phi_{rd} I_{sq} - \Phi_{rq} I_{sd}\right) \qquad (16)$$

Previous researches have shown that rotor defects have influence on the expression of the instantaneous electromagnetic torque (Kral 2000). The spectrum of this instantaneous electromagnetic torque contains signature related to the mechanical fault. Broken rotor bars give rise in the torque's spectrum to a component of frequency 2sf relative to the fault, f being the fundamental frequency and s the slip. The higher the degree of damage, and the greater the load, the more pronounced the characteristic component of the fault in the spectrum of the electromagnetic torque. Figures (7a, 7b, 7c) show the normalized spectrum (in dB) with respect to its mean value, computed from the stator currents and estimated rotor flux in open loop under three different load levels. By this method, the fault characteristic frequency does not appear at low load level (Fig.7 c). Figures (8a, 8b, 8c) show the normalized spectrum with respect to its mean value, computed from the stator currents and rotor flux estimation using Kalman filter under same different load levels. The experimental results related to Kalman method clearly reveal the existence of spectral peaks at 4.88 Hz, 2.44 Hz and 0.7 Hz for full, medium and low load levels respectively. Figures (9a, 9b, 9c) show the normalized spectrum computed from the estimation of rotor flux using extended Kalman filter. Therefore related results to the open loop and EKF show the existence of spectral peaks at 4.88 and 2.44 Hz for full and medium load only. Notice that only the method based on the Kalman filter with the mechanically measured velocity enables the fault detection at low load levels.

3.3. Comparison of several methods

The spectral analysis of the estimated electromagnetic torque computed by different methods shows clearly that when a rotor fault is present, a component appears at the fault's characteristic frequency « f_0 =2sf». f_0 takes the values 0.7 Hz, 2.44 Hz, and 4.88 Hz for low, medium, and full load levels respectively. Kliman (1992) shows that the amplitude of the characteristic frequency is directly linked to the severity of the fault. A criterion "R" is used also to represent the ease of detection of the frequency f_0.

$$R = \frac{\left(P_s - Minl\right) + \left(P_s - Minr\right)}{2} \quad \text{in dB} \qquad (17)$$

P_s is the amplitude of the fault characteristic frequency. *Minl* and *Minr* are the left and right peaks respectively, that have minimum amplitudes around the fundamental peak.

Table 2 Amplitude for specific frequencies & criterions (dB)

Methods	Load	Amplitude at f_0 Healthy Motor (P_0)	Amplitude at f_0 Faulty Motor (P_s)	Criterion Resolution (R)	Criterion (CCT)	Mean (CCT)
E.M. torque computed	Full	-55.5	13.8	48.3	117.6	
from Rotor flux	Half	-28.1	6.6	40.55	75.2	64.28
OL method (w_x=0 rd/s)	Low	0	0	0	0	
E.M. torque	Full	-60.5	2	67.8	130.3	
By KF ; 2nd-order model	Half	-68.5	-24.3	71.9	116.1	93.45
Mechanical frame	Low	-62.1	-64.7	36.4	33.8	
E.M. torque	Full	-59.3	2.41	95.96	157.6	
By EKF ; 2nd-order mode	Half	-65.6	-23.8	55.25	97	105.8
Synchronous frame	Low	-62.8	0	0	0	

A total comparison criterion « CCT» is defined from the amplitude of the fault characteristic frequency (P_s), the characteristic frequency with no rotor imperfections (P_0), and the resolution criterion (R). This criterion is given by the following equation

$$CCT = R + P_s - P_0 \text{ in dB} \qquad (18)$$

The experimental results are presented in Table 2. The mean value of the total comparison criterion « CCT » for the three different load levels reflects method performances to detect a rotor fault. Fig.10 shows the comparison criterion for the three levels of load. In general, methods that make use of flux estimation by a correction step give a better signature for broken rotor bar fault detection. The KF that uses the measured mechanical velocity give best results from low to medium load levels. The EKF is not sensitive to fault detection in case of low load levels, but it gives a great aptitude to detect broken bars at full load.

4. CONCLUSION

This paper has described a new approach for the detection of rotor imperfection by spectral analysis of electromagnetic torque using a standard and an extended Kalman filter. Experimental results using real electric signals show the significance of Kalman filtering to estimate the electromagnetic torque and consequently to detect motor mechanical abnormalities. We have shown that this method can lead to more effective detection of rotor faults even at low load levels. Alternatively, using the EKF allows mechanical velocity estimation. It is an interesting method whilst it allows faults detection without using mechanical sensor.

REFERENCES

Benbouzid M. (2000). A Review of induction Motors signature Analysis as a medium for faults detection. *IEEE Transactions on industrial Electronics* vol. **47** N° 5, pp. 984-993.

Cardoso A.J.M. (1993). Computer-Aided Detection of Airgap eccentricity in operating three phase induction's Motors by park vector Approach. *IEEE Transactions on Industry Applications*, vol. **29** N° 5, pp. 897–901.

Cruz S.M.A & all. (1999a). Rotor cage Fault diagnosis in three-phase induction Motors by the total instantaneous power spectral Analysis. *IEEE Industry Applications conference record*, vol. **3,** pp. 1929-1934.

Cruz S.M.A & all. (2000b). Rotor cage Fault Diagnosis in three-phase induction Motors by Extended Park's Vector Approach. *Electric Machines and power systems* vol. **28,** pp.289-299.

Elkasabgy N.M et all. (1992) Detection of broken bars in the cage rotor of an induction machine. IEEE trans industry Applications, vol **28**, N° 1, pp. 165-171.

El Tabach & all . (2001). Detection of broken rotor bar of induction motors by spectral analysis of the electro-magnetic torque using Luenberger observer *IEEE Industrial electronics IECON'01 27th annual conference, Denver Colorado*, 2001

Kliman G.B Steing. (1992). Methods of motor current signature Analysis. *Electric machines and power systems.* Vol. **20** N° 5 , pp. 463-474.

Kral Christian & all. (2000). Sequences of field-oriented Control for the detection of faulty rotor Bars in induction Machines, the Vienna monitoring method. *IEEE Transactions on Industrial Electronics*, vol. **47** N° 5, pp. 1042-1050.

Stanislaw F. Legoswski & all. (1996). Instantaneous Power as a medium for the signature analysis of induction Motors . *IEEE Transactions on industry Applications* vol **32** N° 4, pp. 904-909.

Trzynadlowski Andrzej & all. (1999a). Diagnostic of Mechanical Abnormalities in induction Motors using Instantaneous electric Power » *IEEE Transactions Energy conversion*, vol. **14** N° 4, pp. 1417 –1423.

Trzynadlowski & all. (2000b). Comparative Investigation of Diagnostic Media for Induction Motors: a case of rotor cage faults. *IEEE transactions on Industrial electronics* vol. **47** Issue 5, pp. 1092 –1099.

Zein Ismail, (2000). In: *Application of the Kalman filter and Luenberger observer to the control of the induction motor.* (Phd thesis in Systems Control, Université de Technologie de Compiègne).